

High-Resolution X-Ray Photoemission from Sodium Metal and Its Hydroxide

P. H. Citrin

Bell Laboratories, Murray Hill, New Jersey 07974

(Received 12 June 1973)

X-ray photoemission spectra of valence and core electrons in sodium and sodium hydroxide were measured from clean and oxidized sodium-metal films. Clean metal surfaces were prepared by sequential evaporation, with the resultant films contaminated by less than half a monolayer of impurity after 8 h running time. From these films an analysis of line shapes of core-electron spectra has revealed, for the first time in x-ray photoemission, evidence for the effects of electron-hole interactions as discussed by Mahan and by Nozières and de Dominicis. The valence band of sodium metal was measured and found to be free-electron-like with an occupied bandwidth in good agreement with theory. Accurate values of binding energies for the core Na $2p$, $2s$, and $1s$ electrons are found to be 30.58 ± 0.08 , 63.57 ± 0.07 , and 1071.76 ± 0.07 eV, respectively. Through comparison with core-level spacings in the free ion and crystal, it was inferred that the $2s$ and $1s$ electron binding energies in the metal are anomalously large. It is argued that this result is opposite to that expected from polarization energy arising from differences in nuclear-charge screening for different core electrons. Furthermore, it is noted that this effect is evident in metals other than sodium. The valence band of sodium hydroxide was measured and shown to very closely resemble the measured valence band of water vapor after shifting the vapor spectrum to lower absolute binding energies. This shift incorporates differences in reference levels and initial-state potentials for the gaseous and solid species and also includes the electronic polarization of the ions in the crystal following photoionization. Analysis of core and valence regions coupled with appreciably smaller binding-energy shifts with phase change helped identify molecular nitrogen very weakly chemisorbed on the NaOH surface.

I. INTRODUCTION

The alkali metals, by virtue of their essentially free-electron-like behavior and simple monovalent electronic structure, have been the subject of theoretical investigations for over forty years.¹ The properties that account for their theoretical interest are quite naturally responsible for their experimental appeal as well. It is for these reasons that an investigation of such basic phenomena as electron binding energies and many-electron effects in metals was undertaken in such a system.

X-ray photoelectron spectroscopy was used for this study, a technique that has been shown to provide accurate electron-binding-energy data for those systems in which sample charging is not a problem.^{2,3} Furthermore, with the advent of relatively monochromatic x radiation and improved vacuums and sample preparations, it is now possible to obtain low-background high-resolution data on systems previously too reactive to investigate. The sodium system was chosen as a compromise between lithium with only two core electrons available for theoretical comparisons, and the remaining alkalis which, because of their volatility in the high-vacuum-region required, necessitate special cooling procedures. In the next section, we describe the experimental procedures taken to obtain clean metallic-sodium surfaces. Our procedures, while quite effective, are significantly less elaborate than those described by other workers.

II. EXPERIMENTAL PROCEDURE

The data reported here were taken with the HP 5950A ESCA spectrometer. The instrument, using bent quartz crystals coupled with the technique of dispersion compensation,⁴ provides relatively monochromatic $AlK\alpha_{1,2}$ x radiation for higher resolution and lower background due to the lack of bremsstrahlung. The spectrometer also has the capability of achieving ultra-high vacuum, but in order to do so, modifications are required. Because the vacuum system is of particular concern to those systems that demand clean surfaces, we describe below the modifications we have made in these experiments.

As delivered, the vacuum system is comprised of three, separately pumped systems: the x-ray chamber, at a typical working base pressure of 4×10^{-9} torr, the energy-analyzer region, at a nominal working base pressure of $< 10^{-9}$ torr, and finally the sample-preparation chamber. The vacuum in this last region is most critical for it is here in which samples are cleaned and, when appropriate, evaporated. The three separate platelets onto which samples are externally mounted or internally evaporated are introduced into this region via a rather long (~ 70 cm) polished rod which slides through Teflon seals; these, in turn, are continuously pumped to about several millitorr to provide differential pressures between the sample chamber and atmosphere. The evaporating cross

probe or rod, containing within itself a cavity in which sits a double-stranded tungsten-wire helix, slides transversely to the sample-holder rod through similarly pumped Teflon seals. The weakest links in the entire vacuum system are clearly these seals, because upon movement of the rods, small quantities of air through the seals and adsorbed moisture on the rods are introduced into the sample preparation chamber. A recent effort to deal with these problems has involved replacing the sample insertion and evaporation mechanisms with a closed, continuously pumped system which is mechanically operable from outside.⁵ In an effort to investigate the limits of other, more simple approaches we have made the following modifications which, by the above standards, are quite unsophisticated.

Around both the sliding cross-evaporating and platelet-holding probes were secured individual glove bags, one of which containing vacuum-sealed vials of sodium (99.999%)⁶ and appropriate equipment for handling. After the bags were repeatedly purged with refrigerated dry nitrogen, a sodium charge was quickly placed into the helical boat and then introduced into the sample-preparation chamber. At the onset of the first, rapid evaporation onto polished stainless-steel substrates, the base pressure of 4×10^{-8} torr quickly rose to 1×10^{-7} torr and then quickly returned to base pressure. The sample was then inserted into the energy-analyzer region and its purity analyzed from its photoemission spectrum (see Sec. III). Subsequent evaporations raised the base pressure now $\sim 10^{-8}$ torr to only $\sim 4 \times 10^{-8}$ torr and resulted in increasingly pure surfaces. The valence region of sodium required an 8-h run and was recorded following the final evaporation. After this run, the sample rod was retracted into the nitrogen-gas-filled bag until the films were visibly oxidized and the samples were then reanalyzed. The x-ray photoemission results and discussion of the evaporated metallic and oxidized sodium films are given in the sections below.

III. SURFACE PURITY

Bearing in mind that x-ray photoemission is essentially a surface technique ($\sim 10\text{--}20 \text{ \AA}$),⁷ the purity of the surfaces from which the photoelectrons are ejected must be ascertained before inferring any information about metallic sodium. The most sensitive and direct method available to us is to monitor *in situ* the contaminant core photoemission lines of the most obvious offenders, namely, carbon and oxygen in the probable forms of CO, CO₂, O₂, and H₂O. Carbon impurities were observed to be relatively insignificant in these experiments and are briefly discussed in Sec. VI. The oxygen contamination, on the other hand, was observed

to be important and so O 1s spectra were investigated under a variety of conditions. These spectra are shown in Fig. 1. The upper-most spectrum, Fig. 1(a), is of O 1s electrons taken 30 min after the first successful evaporation of sodium metal. During this 30-min time, three scans (100 sec/scan) of the Na 2s electrons were recorded, followed by about 25-min data-accumulation time of Na 2p electrons. During the next 60 min and after the O 1s spectrum above was taken, Na 1s and Na 2s electrons were recorded. The oxygen 1s region scanned after these additional runs is seen in Fig. 1(b). Following another evaporation from which the sodium core electrons were rerun as a check on the reproducibility of the first runs, the final evaporation was performed, and the valence band region was recorded. The oxygen 1s region analyzed upon completion of this run is shown in Fig. 1(c). Lastly, in Fig. 1(d) we show the O 1s region recorded after the last evaporated film was exposed to the nitrogen gas in the sample-holder glove bag.

Inspection of these spectra shows that the higher-binding-energy signal associated with the exposed, more heavily oxidized sodium species, Fig. 1(d), is barely present in the first evaporation after 30 min, Fig. 1(a), but grows with time and is clearly present after 90 min, Fig. 1(b). By the last evaporation, Fig. 1(c), it is barely perceptible even after 8-h exposure in the analyzer-region vacuum. Based on the photoemission spectrum of the valence electrons in the oxidized species (see Sec. VI), we assign this higher-binding-energy component to O 1s electrons in NaOH. The sodium hydroxide is understood to arise from the gettering by the sodium metal of the water vapor present in the adsorbed and diffused moisture in the plastic glove bag. The rather long time required for observance of this peak even in the first evaporation is some indication of the relatively low *partial* pressure of the water vapor present in the vacuum system at that time.

The peak appearing at about 1.2 eV lower binding energy to the O 1s line is the ¹P multiplet component of the Na KLL Auger manifold. Discussion of the Auger spectra in both Na and NaOH will be given in a separate work.⁸ In the meantime we can say that oxygen contamination associated with our sample preparation procedures is in evidence even on the high inelastic background of sodium Auger electrons. Because it is desirable to get some idea of the degree of contamination imposed in these experiments, it is tempting to compare our data with the ultra-high-vacuum x-ray photoemission data on Al metal, reported very recently by Baer and Busch⁹ and by Barrie.¹⁰

In the former work the O-1s-to-Al-2s intensity ratio (measured with MgK α radiation) was stated

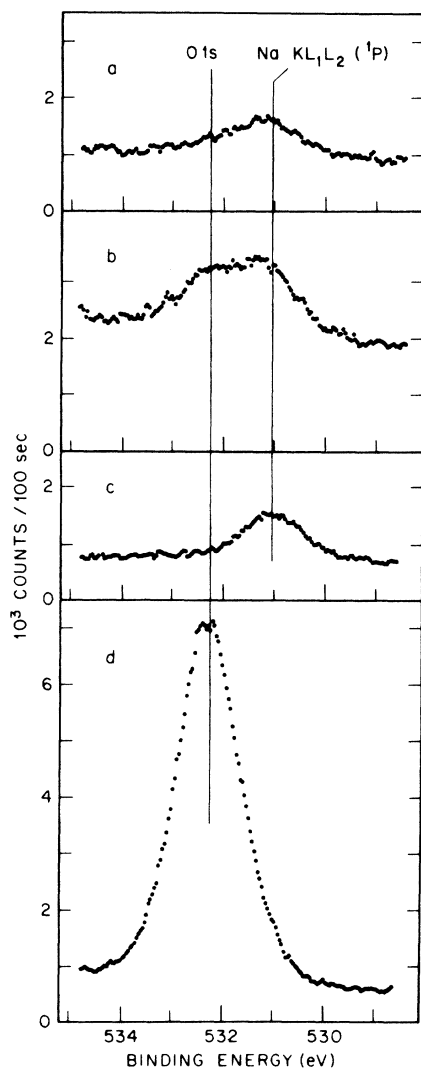


FIG. 1. Photoemission spectra of O 1s electrons recorded under various experimental conditions. Spectra were obtained following (a) 30 min of analysis (first evaporation), (b) 90 min analysis (first evaporation), (c) 8 h analysis (third evaporation), (d) exposure of (third) evaporated sodium film to partially moist nitrogen atmosphere. Scanning time is the same for all cases shown.

to be less than 0.01. In the latter work, no relative intensity data were reported but from the raw data (taken with $AlK\alpha$ radiation) we estimate that same ratio to be between 0.10 and 0.15. We note that while these ratios are, in general, qualitatively useful for comparison between different experiments on the same material, they do not convey information regarding the actual relative quantities of contaminant and metal. This follows for two reasons. First, the mass absorption coefficients for materials of different atomic number Z are roughly proportional¹¹ to Z^4 assuming, of course, they are on the same side of the absorption edge of

the exciting radiation. Aluminum and oxygen have not only different atomic numbers but are also on opposite sides of the Al and Mg K absorption edges. Second, the total mass absorption coefficient is composed of the individual attenuation coefficients for the various atomic subshells; O 1s electrons, for example, have much larger photoelectric cross sections than do O 2s electrons. Therefore, in comparing relative intensities to learn about relative quantities, one must take account of these points.

With reference to the present system, it is meaningful to compare the relative intensities of Na 1s and O 1s electrons since these species are on the same side of the Al K edge and are, for all practical purposes, isoelectronic (the Na 3s photoelectric cross sections are negligibly small). Using the integrated areas determined from least-squares fits (discussed in Sec. V) for the O 1s peak in the most contaminated case for sodium metal [Fig. 1(b)] yields an O-1s-Na-1s ratio of 0.013; after the appropriate Z^4 correction,¹¹ this becomes 0.047. To determine how thick this oxygen contamination layer is, we must know the escape depths of O 1s and Na 1s photoelectrons. Tracy¹² has shown that to a first approximation, electron escape depths depend primarily on their kinetic energy and are relatively insensitive to their environment above kinetic energies of about 20 eV. Sodium 1s and oxygen 1s electrons photoejected with $AlK\alpha$ radiation (~ 1500 eV) have kinetic energies of about 400 and 1000 eV, respectively, corresponding to approximate escape depths of 8 and 14 Å. We see from these values that the amount of oxygen contaminant for this case [Fig. 1(b)] is only a very small fraction, $\sim 10\%$, of a monolayer.¹³ This result, however, appears to us to be too small. The reason for this lies in our value used for the escape depth of sodium; if correct, it corresponds to an effective sampling depth in our experiment of only about two monolayers, or about a factor of 3 or 4 smaller than that in most metals.¹² This rather large discrepancy results from the anomalously low density of sodium relative to the densities of most other materials. If we assume the escape depth of electrons in sodium is about four times larger, the thickness of the oxygen-containing layer is estimated in this worst case to be about 40% of a monolayer, still a satisfactory result when viewed with our unelegant but rather facile sample preparation procedures.

IV. SODIUM VALENCE BAND

The sodium valence band spectrum was analyzed from a freshly evaporated film following two prior evaporations, as described above. Of significance in this run is the fact that the sodium surface was particularly free of the oxygen impurity associated

with the heavily oxidized sodium. This was determined through analysis of the core, rather than the valence region of oxygen because the low cross sections for x rays of the valence orbitals make their detection time consuming. Also, in the absence of controlled surface contamination procedures, surface purity inferred from valence orbital intensities may be somewhat misleading. As will be seen in Sec. VI, this is especially true for sodium, in which a single strong bulk-plasmon loss at about 5.8 eV obscures the $2a_1$ and $1b_1$ hydroxide molecular orbitals effectively, while the more intense $1b_2$ molecular orbital appearing at about 11.0 eV could erroneously be assigned as a second plasmon loss.

Several features of the spectrum, shown in Fig. 2, deserve comment. The shape of the valence band closely resembles the free-electron parabola. This is not too surprising for it is well established from a variety of Fermi-surface measurements that sodium is the most free-electron-like alkali metal.¹⁴ The width of the occupied part of the band, calculated from the free-electron model using $r_s = 3.99$ a.u., is 3.18 eV. We have least-squares-fitted our data with a parabola and determined the width of the occupied band to be about 3.2 ± 0.1 eV, in very good agreement with theory. It should be mentioned that in the fit, shown in Fig. 2, we have not subtracted the small inelastic background on the high-binding-energy side of the band. To assess the importance of this procedure, the spectrum was also fitted with a parabola after having subtracted a sloping linear background passing through the uppermost portion of the inelastic tail, as shown in Fig. 2; the width of the occupied band was then determined to be about 2.8 ± 0.1 eV. Since

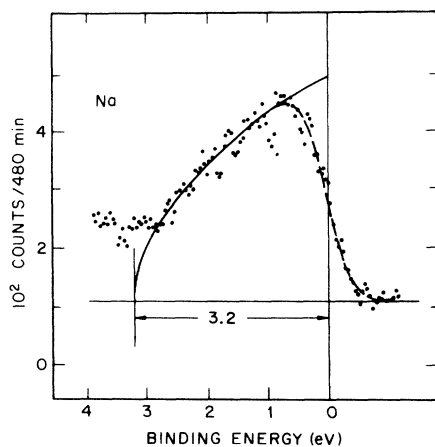


FIG. 2. Sodium valence band photoemission spectrum. A least-squares fit for the free-electron parabola is shown by a solid line superposed on the raw data. The rounded Fermi edge determined by spectrometer resolution and the inelastic tail at higher binding energy are also seen.

both of these procedures represent upper and lower limits, we may safely quote the average of 3.0 ± 0.2 eV as being a reasonably reliable value for the occupied bandwidth. The precision of the aforementioned technique is limited not only by the magnitude and shape of the subtracted background, but also by the determination of the position of the Fermi edge. This uncertainty is, however, quite small for metals with well-defined edges and we estimate it for sodium to be between 1–2 channels (0.04 eV/channel). The roundedness of the edge is due to the instrumental resolution (~ 0.5 – 0.6 eV), while temperature broadening contributes only a few hundredths of a volt.

We comment here that these limitations imposed by the x-ray-photoemission (XPS) technique in studying the valence band (density of states) are far outweighed by its advantages, especially when compared with the other available methods, e.g., ultraviolet photoemission (UPS) and soft-x-ray spectroscopy (SXS). Briefly,¹⁵ UPS has resolution superior to that of XPS, but is plagued by (a) very low sampling depths, making the technique especially surface sensitive, and (b) final states whose band structure obscures the density of initial states. SXS, on the other hand, does not have these problems, but instead must contend with measuring the shape and width of both the valence and the core level to which the valence electron decays. Since all three techniques must subtract an inelastic background, XPS, which measures the density of occupied states directly (matrix-element modulation is, in general, not important),^{9,15} seems to be the most straightforward technique for these kinds of measurements.

V. SODIUM CORE ELECTRONS

A. Results

The photoemission spectrum of Na $2p$ electrons taken after the first successful evaporation is shown in the upper half of Fig. 3. There are three kinds of lines drawn in this figure. The solid curve represents the result of a nonlinear least-squares fitting procedure, which uses line shapes adjustable between Gaussian and Lorentzian and an adjustable linear background. It is solid up to and including the data points used in the actual fit. The long-dashed line following from this solid one is the computer drawn extension of the peak, fitted with the constraints determined from the solid portion. The short-dashed peaks are the $2p_{3/2}$ and $2p_{1/2}$ spin-orbit components comprising the fitted $2p$ line. The only parameters constrained in the fit were the relative areas of the multiplets (2:1), and their energy separation of 0.169 eV taken from atomic data.¹⁶ In Fig. 3 is also seen a sloping background which is simply due to in-

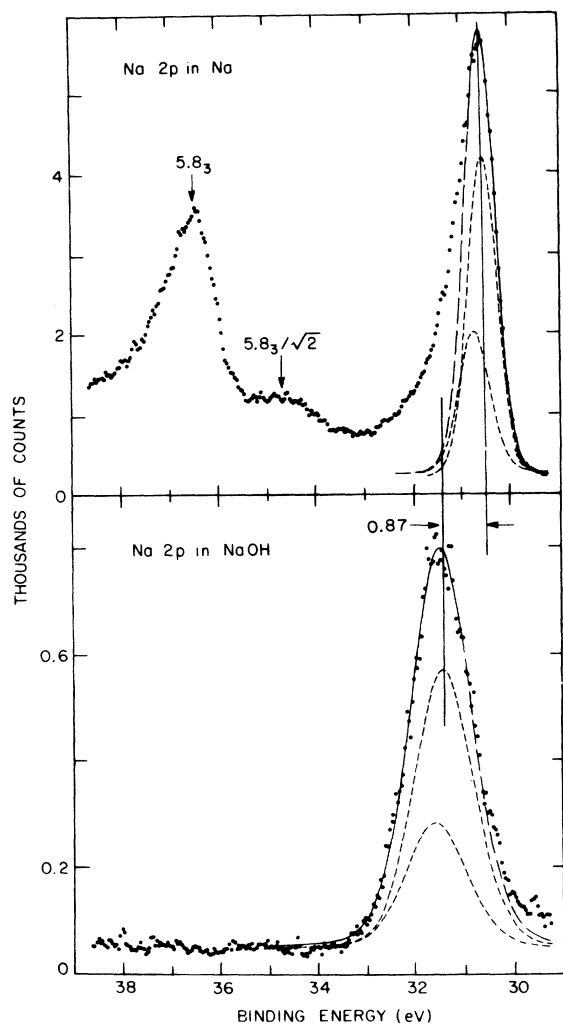


FIG. 3. Sodium $2p$ electrons in metal and hydroxide. Solid plus long-dashed lines represent computer-drawn nonlinear least-squares fits. Short-dashed lines are $2p_{3/2}$ and $2p_{1/2}$ components of fitted peaks. Note the presence of the first bulk plasmon and surface plasmon superposed on inelastic tail in the metal and their absence in the hydroxide. The hydroxide Na $2p$ peak is chemically shifted from metal by 0.87 eV.

elastically scattered photoelectrons emerging from the sample. The importance of this background varies for different core electrons because upon photoejection, their kinetic energies, and therefore their scattering cross sections, change. This is most clearly seen by comparing the inelastic tail of Na $2p$ electrons in Fig. 3 with that of Na $1s$ electrons in Fig. 5. In any event, if this background is subtracted, the fitted peak positions (not their widths) change by no more than 0.03 eV; in order to present the raw and fitted data compactly, we have simply shown the peaks fitted with a constrained linear background.

Returning to Fig. 3 we see superposed on the inelastic tail the first bulk-plasmon peak appearing at a lower kinetic energy from the weighted average of the main peak by 5.83 ± 0.06 eV (errors are discussed below). This value appears to be in excellent agreement with 5.85 ± 0.1 eV observed by Swan,¹⁷ and in only fair agreement with 5.71 ± 0.1 eV reported by Kunz.¹⁸ The surface plasmon, as predicted by theory,^{19,20} is also indicated in the figure. The good agreement between experiment and theory of the surface-plasmon peak position is interpreted as further evidence of the surface cleanliness.²⁰

Following the above run and the subsequent O $1s$ run, the Na $2s$ electrons were analyzed and are shown in the upper half of Fig. 4. The same solid- and dashed-line notation as in Fig. 3 is used here. Comparison of this with the Na $2s$ spectrum run immediately upon introduction into

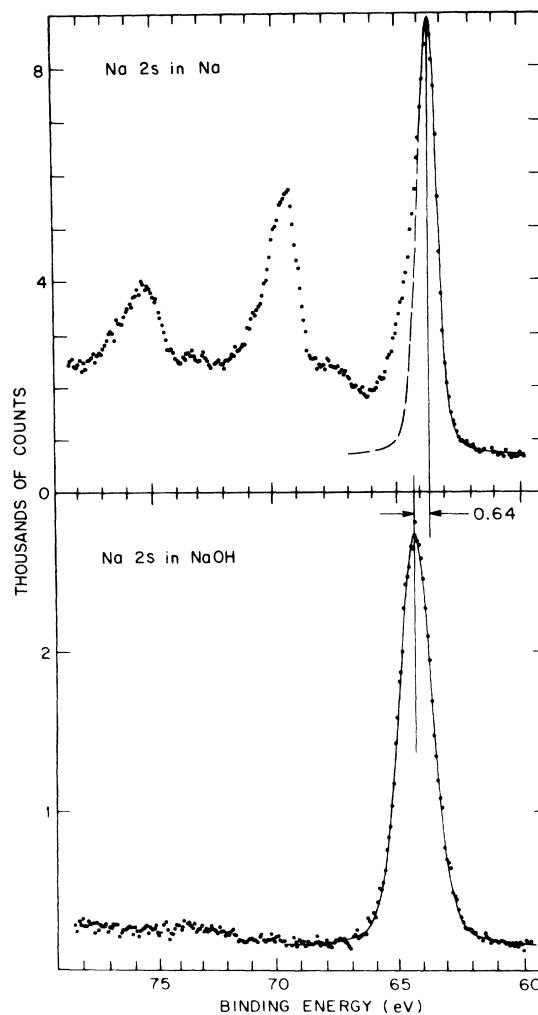


FIG. 4. Sodium $2s$ electrons in metal and hydroxide. See Fig. 2 caption for details.

the analyzer region showed them to be virtually identical.

The Na 1s electrons were recorded from a subsequent evaporation and are shown in Fig. 5. On top of the considerably extending inelastic tail are four easily observable bulk-plasmon replicas. The surface plasmon S and the surface- plus bulk-plasmon peak $1+S$ are also indicated.

Values of the magnitudes of the sodium core-electron binding energies are given in the first column of Table I. They were all determined by the described least-squares fitting procedure after subtraction of the inelastic background. These numbers are given relative to the Fermi level and thus are not absolute binding energies in the convention of defining the binding energy of the vacuum level as zero. To make these values absolute in this sense requires an accurate knowledge of the work function for sodium. At present, the best data available to us for polycrystalline sodium are given by Oirschot, Brink, and Sachtler,²¹ whose value of 2.36 ± 0.02 eV is within experimental error of 2.38 eV reported by Malov, Lazarev, and Salov.²²

In Table I, the numbers in parentheses represent the uncertainties in the last digit. These incorporate by statistical laws the sum of uncertainties associated with (i) determining the peak position by our least-squares fitting procedure, typically 0.01 to 0.02 eV, (ii) defining the position of the Fermi level, ~ 0.06 eV, and (iii) the experimental drift of the spectrometer. This last quantity is estimated to be no more than a few hundredths of an eV based on the high reproducibility of the positions observed during the course of these experiments for the same peak, as determined from least-squares fit. Although the absolute values

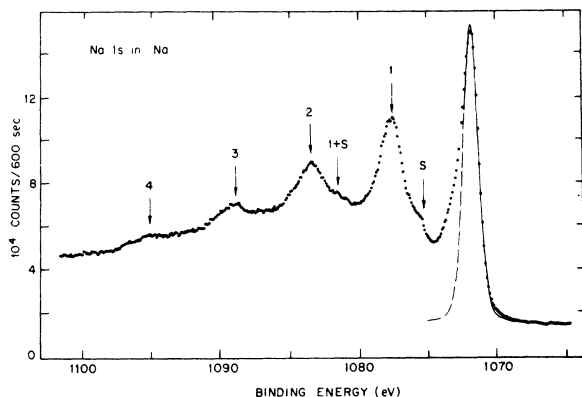


FIG. 5. Sodium 1s electrons in metal. Superposed on extended inelastic tail are four bulk-plasmon loss peaks. Surface plasmon (S) and bulk plus surface plasmon losses ($1+S$) are also indicated.

TABLE I. Sodium-electron binding energies (eV) relative to the Fermi level.^a

	Na	NaOH ^b	Δ^c
Na $2p_{3/2}$	30.52(8)	31.39(9)	0.87(6)
Na 2s	63.57(7)	64.21(8)	0.64(6)
Na 1s	1071.76(7)	1072.59(8)	0.83(6)

^aNumbers in parentheses correspond to uncertainties in the last digit. Sources of error for values in the first two columns are discussed in the text.

^bThe exact position of the Fermi level in NaOH is unknown (see text).

^cThe chemical shift. Values in parentheses correspond to uncertainties in the last digit and are determined from the difference between the first two columns according to statistical laws. The constant error in determining the Fermi edge for either metal or hydroxide is not included.

of the core binding energies may be uncertain by as much as 0.08 eV, their relative positions are, of course, more precisely determined.

In the discussion given below, we divide our attention into two areas: the line shapes and the line positions of metallic-sodium core electrons. With regard to the latter, we shall focus not so much on *absolute* metallic core-electron binding energies here, but rather on comparing their *relative* spacings with those of atomic, free-ionic, and ionic-crystal data. A detailed discussion of the absolute values of core-electron binding energies and the calculation of them using pseudopotentials and a *nonlinear* response theory will be given in a separate work.⁸ An application of this theory has been recently reported in the calculation of binding energies of electrons in rare gases implanted in noble metals.²³ In Sec. V C below we shall only impart a flavor for the terms included in this theory.

B. Line Shapes: Evidence of Many-Electron Excitations by Core Holes

Inspection of the line shapes of those core electrons shown in Figs. 3–5 shows them to be asymmetric, exhibiting a rather large broadening on the higher-binding-energy side. Even after subtraction of the inelastic background the asymmetry is quite appreciable, as shown in Fig. 6. It is for this reason that only an incomplete portion of the peak was used in the actual least-squares fits. From Fig. 6 it is seen that the asymmetry is largest for Na $2p$ electrons and smallest for Na 1s electrons. Considering just the case of Na $2p$, the cause for the asymmetry could be simply due to the presence of oxidized sodium, as is suggested by comparison with the oxidized form shown in the lower half of Fig. 3. If the intensity

(integrated area) of the fitted symmetric main peak is subtracted from that of the entire asymmetric peak, it is seen that the asymmetric tail contributes almost 30% to the total intensity. However, we have shown in Sec. III that the oxygen contamination at this time [Fig. 1(a)] was less than 5% of the total intensity. Moreover, if this broadening were due to oxidized surface impurities, the relatively cleaner Na $2p$ [Figs. 1(a) and 3] would exhibit a smaller contribution than that observed for the case of Na $2s$ electrons for which the impurity accumulation was observed to be greater [Figs. 1(b) and 4]; in point of fact, the asymmetric contribution is significantly larger for the Na $2p$ spectrum (Fig. 6). A further argument for ruling out surface contamination as a primary cause is based on the opposite trend of observed asymmetry with escape depth: Na $1s$ electrons, while having the shortest escape depths and thus the greatest sensitivity to surface impurities, exhibit the smallest degree of asymmetry. Finally, the possibility of this broadening arising from the folding of an asymmetric spectrometer contribution into an otherwise symmetric line shape is also ruled out on the basis of the very narrow and symmetric photoemission peaks observed for Au $4f$ electrons in Au metal. Thus the major portion of the asymmetric tail is still left unaccounted.

We believe the source of this tail to be due to excitations of the conduction electrons by the sudden creation of the core hole immediately following photoionization. This many-electron behavior was first discussed by Mahan,²⁴ and later by Nozières and de Dominicis,²⁵ in explaining the effect of the final state interactions on the shape of the soft-x-ray emission edge in metals. Following these works Doniach and Šunjić,²⁶ among others,

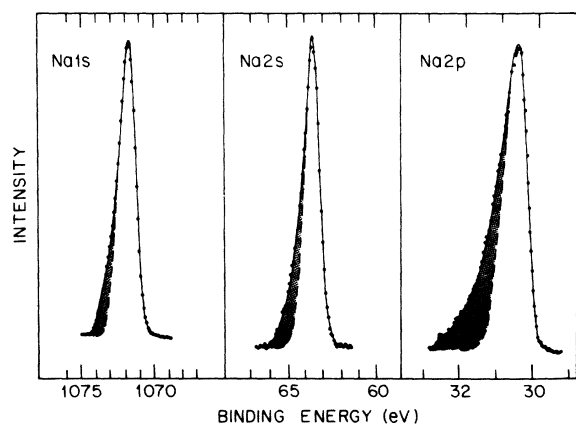


FIG. 6. Evidence for conduction-electron excitations from core holes. The effect, shown as shaded asymmetric broadening, is more obvious for the narrower peaks of the long-lived core electrons. Note the different energy scales for each core electron.

have predicted that this behavior should reveal itself in x-ray photoemission spectra as asymmetric broadening of core-electron lines.

The observation of this effect in XPS spectra of metals has been heretofore unnoticed for at least two reasons. The first is that the resolution required to see this asymmetry has not been previously realized by conventional nonmonochromatic x-ray sources. The second reason is that, even with adequate experimental resolution, there is still linewidth broadening due to the inherent lifetime contribution of the core hole. It is therefore not surprising that after the inelastic background is subtracted from the Na $1s$ spectrum, the asymmetry of the resulting core line is significantly smaller than that for the relatively long-lived Na $2p$ electrons. Since the degree of electron-hole coupling varies in different metals and the effects of such coupling in XPS is quite different from that in SXS,^{26,27} it should be most interesting to investigate further this kind of behavior in other free-electron-like systems.

C. Relative Core-Level Spacings in Atom, Ion, Crystal, and Metal

One of the basic tenets in photoelectron spectroscopy is that while changes in valence electron distributions cause absolute binding energies of core levels to vary, core-level spacings are invariant to such modifications, regardless of their environment. To test this assertion critically, accurate and precisely determined experimental values are required. In Fig. 7 we present the data pertinent for this test. All values of a particular configuration shown in this figure are weighted averages of the multiplets or spin-orbit components in that configuration. A point of clarification in the discussion below (as well as in those already presented) is that the binding energy of a particular electron shall always be considered in terms of its absolute magnitude. Thus Na $2s$ electrons have greater binding energies, i. e., ionization potentials, than do Na $2p$ electrons.

We lay the ground work for our discussion by first comparing the $2p$ -electron binding energy in the free Na (I) ion (FI) and the free atom (FA). These electrons are less bound in the atom than in the ion as a result of two effects. The first is simply the change in the initial-state Hartree potential, $\Delta V_{FA} \equiv V_{FI} - V_{FA}$. The second, a final-state effect, is the polarization energy of the $3s$ electron in the atom by the $2p$ hole. (There is, of course, polarization of the other electrons present for both the atom and ion cases, but we are now just talking about differences.) Hedin²⁸ has calculated both these effects for Na, as well as for Li, K, and Al, using Hartree-Fock and linear-response theory. He finds the change in initial-

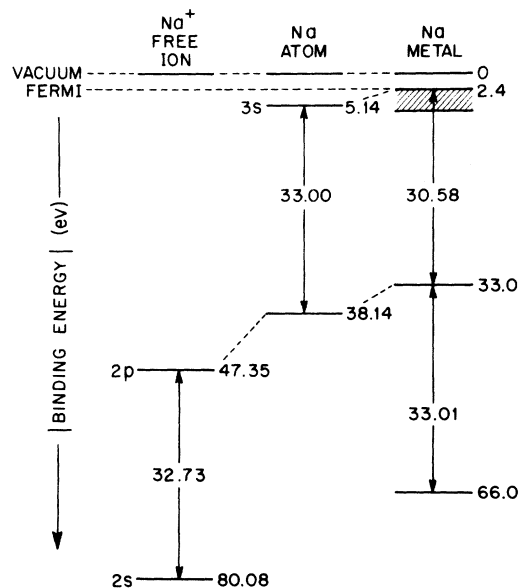
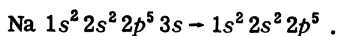
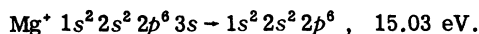


FIG. 7. Comparison of energy levels and splittings of electrons in free sodium ion [Na (I)], sodium atom, and sodium metal. Absolute magnitude of binding energy increases towards the core.

state potential ΔV_{FA} for Na $2p$ electrons to be about 12.7 eV, while the change in polarization energy for these electrons due to the presence of the $3s$ electron in the atom to be about 1.3 eV. The sum of these numbers is in good agreement with the experimental¹⁶ value of 14.35 eV for the process



We note that this result is an explicit demonstration of the breakdown of the "equivalent core" approximation, which states that the core of a species of atomic number Z containing a core hole is approximately equivalent to the core of the isoelectronic species of atomic number $Z+1$. In this case, the ionization of a $3s$ electron from a sodium atom with a (core) $2p$ hole should be closely approximated by the process



The discrepancy of about 0.7 eV must be interpreted as arising from the inability of a $2p$ electron to screen one unit of nuclear charge near the nucleus.²⁹

In this regard, it would be interesting to have accurate experimental $2s$ and $1s$ ionization potentials for atomic sodium in order to assess the importance of screening on electron binding energies. This follows because the screening effect should have significance in determining the change in polarization energy for different core electrons: the larger the screening of a particular core state, the greater the polarization power

of that state's hole and thus the lower its binding energy. In the absence of atomic data, we would expect the measured core-level spacings of electrons in solids to reflect any differences in screening. However, before turning attention to the metallic case to see if this is true, it is necessary to summarize briefly some results for the case of an ionic crystal.

In such a system it was shown that the binding energy of the i th electron on the j th species in a crystal, $E_X(i,j)$, or in a free atom, $E_{FA}(i,j)$, may be expressed by³⁰

$$E_X(i,j) = E_{FA}(i,j) + q_A e^2 / r_i + q_i e^2 \Phi_j / R + E_{rep}(j) + E_{pol}^X(j) + \Delta W_X . \quad (1)$$

Here q_A is the charge added to or removed from an average radial distance r in the j th free atom, Φ_j is the Madelung potential of the j th ion in the crystal with interionic distance R and composed of ions with charge q_i , $E_{rep}(j)$ is the repulsive energy experienced in the crystal by the j th ion, and ΔW_X (the contact potential) is the difference between the work function of the crystal and the spectrometer, $W_X - W_{sp}$. This last term is added to the expression so as to reference the crystal binding energies to its vacuum level. The crystal polarization energy of the j th hole-state ion, $E_{pol}^X(j)$, accounts for the polarization of the electrons localized on all the other surrounding ions in the lattice. The term is a negative quantity because the polarized electrons partially screen the charge on the hole-state ion from the ejected photoelectron, thereby effectively lowering its binding energy.

If we assume the crystal to be completely ionic, then $q_A = q_i = n$ ($n = \text{integer}$), and the first and second terms are simply equal to the free-ion electron binding energy. The third and fourth terms represent the change in potential energy in going from the free ion to the ion in a crystal, i.e., $\Delta V_X \equiv V_{FI} - V_X$. Equation (1) may now be rewritten as

$$E_X(i,j) = E_{FI}(i,j) + \Delta V_X(j) + E_{pol}^X(j) + \Delta W_X . \quad (2)$$

From this expression it is seen that core energy-level spacings in the crystal should be equal to those in the free ion, a result that has been confirmed in a variety of ionic systems.^{30,31} The measured Na- $2p$ -Na- $2s$ splitting in NaOH of 32.76 ± 0.06 eV (weighted Na $2p$) (see Table I and Sec. VI below) compared with a free-ion splitting of 32.73 eV¹⁶ is further corroboration of this prediction. Implicit also in these results is that the crystal polarization energy is independent of what core electron is ejected. [The polarization energies for the various core electrons in the free ion itself are, of course, different but this is already accounted for in the first term of (2).]

We are now in a position to discuss our results

for the case of sodium metal. In general, the binding energy of the i th electron in a metal may be expressed by

$$E_M(i, j) = E_{F1}(i, j) + \Delta V_M(j) + E_{po1}^M(j) + \Delta W_M. \quad (3)$$

As written, (3) is analogous to (2) in both form and notation, e.g., $\Delta V_M \equiv V_{F1} - V_M$. Here, as in the case of the crystal, the vacuum level is the zero energy reference.

The most straightforward prediction of Eq. (3) is that the core energy-level spacings in the metal, as in the crystal, should be equal to the corresponding splitting in the free ion. In Fig. 7 it is seen that this simple prediction is in disagreement with experiment by almost 0.3 eV, certainly outside the limits of experimental error. We argue below that this discrepancy cannot be accounted by differences in nuclear charge screening; further on we shall also show that the size of this discrepancy is actually larger than it appears.

By an ionization scheme analogous to that presented above for the free atom, we may think of an atom in a metal as being ionized in two steps. In the first, a core electron from a free Na (I) ion is removed; in the second, the photoionized ion is surrounded by not one 3s electron as in the case of the atom, but *two* 3s electrons. The reason for this is that in the metal, the mobile conduction electrons are quickly polarized by the core hole and relax accordingly to screen the hole from the ejected electron.^{8,23} (In this vein it is interesting to note that Wolff *et al.*³² have recently observed transitions in atomic sodium corresponding to $2p^6 3s^2 S_{1/2} - 2p^5 3s^2 P_{3/2, 1/2}$ that are within a few tenths of a volt of the 2p electron binding energy we observe in the metal.) If core screening in this "free metal ion" was significantly more effective for 2s than for 2p electrons, the polarization energy would be larger for the 2s electrons, resulting in a *smaller* 2s-2p spacing. This is just opposite to what is observed.

It would, of course, be interesting to see if this behavior is exhibited for other core levels and in other metals as well. A simple way such information may be inferred is the following. We have shown above that to a good approximation, core level spacings of ions in an ionic crystal are equal to those in the free ion. Assuming a salt of a metal to be ionic, it should be possible to deduce changes in core level splittings between the metal and the free ion through comparison of the metal-metal-salt chemical shifts for different core electrons. This may be seen by subtracting Eq. (3) from (2), giving

$$(E_X - E_M) = (\Delta V_X - \Delta V_M) + (E_{po1}^X - E_{po1}^M) + (\Delta W_X - \Delta W_M). \quad (4)$$

We have omitted the index identifying the species involved because we are just considering a metal and its cation. The last term in (4) is of course constant for all core levels. Subtracting the remaining terms for the i th inner core and the j th outer core electron gives, upon rearrangement, the *difference* in core level spacings between a crystal and a metal,

$$\begin{aligned} & [E_X(i) - E_M(i)] - [E_X(j) - E_M(j)] \\ &= [E_X(i) - E_X(j)] - [E_M(i) - E_M(j)] \\ &= \{[\Delta V_X(i) - \Delta V_X(j)] - [\Delta V_M(i) - \Delta V_M(j)]\} \\ &+ \{[E_{po1}^X(i) - E_{po1}^X(j)] - [E_{po1}^M(i) - E_{po1}^M(j)]\}. \quad (5) \end{aligned}$$

Let us ignore for the moment the first term in curly brackets in (5), leaving just the differences in polarization energies. We have argued above that the left-hand side of (5) should be positive if polarization changes due to screening are important or zero if they are not (recall that polarization energies are negative quantities). As an illustrative case, we consider Na and NaOH with the very good assumption that the Na-OH bond is ionic. In the third column of Table I the chemical shifts between Na 2s and Na 2p electrons indicate the left-hand side of (5) is negative, viz., -0.2 eV. We note that this behavior is not peculiar to sodium. Barrie¹⁰ has recently measured the chemical shifts between Al and Al₂O₃ to be 2.4 ± 0.1 eV for Al 2s electrons and 2.7 ± 0.1 eV for Al 2p electrons, again the same trend as observed in sodium.

If we now compare chemical shifts of Na 1s and 2s electrons, however, the trend reverses itself. The implications of this result are quite interesting. We have stated that differences in nuclear-charge screening between 2s and 2p electrons might be expected to be significant in possibly *decreasing* the 2s-2p level spacings, but because atomic data were lacking for 2s electrons we could not determine its importance; since the 2s-2p spacing *increased* in the metal, it seemed to indicate that this effect was negligible. However, the difference in screening between 1s and 2s or 2p electrons is well established,^{33,34} and therefore we certainly would have expected the polarization energy for 1s holes to be larger, i.e., the 1s electron binding energies to be lower by a greater amount in the metal. That we observe essentially the same change in binding energy for 2p and 1s electrons in going from the ion, bound or free, to the metal seems to indicate that some other effect is at play which just cancels the screening effects for 1s electrons. For the case of 2s electrons, this canceling effect dominates any possible screening effects, with the result that the (anomalously) larger 2s-electron binding energies in the metal are more apparent.

We have thus argued that *final-state* polarization

effects should produce smaller spacings in the metal than in the crystal (\approx ion). At this point the source to look for the apparent canceling effect would naturally be in the term in (5), ignored above, which incorporates *initial-state* differences in potential energy shifts. However, inspection of Hartree-Fock energies for different core electrons in the ion and the atom²⁸ show the *difference* of their *spacings* to be essentially unchanged, so it seems reasonable to assume that they are not responsible for the unexpectedly larger 1s and 2s electron binding energies in the metal. The explanation of this effect is, therefore, presently not known and further work is needed to determine its origin.

VI. VALENCE AND CORE ELECTRONS OF SODIUM HYDROXIDE

Some of the results of the oxidized sodium film have already been discussed. Photoemission spectra of the Na 2*p* and 2*s* electrons from this film are shown in the lower halves of Figs. 3 and 4, respectively, while the O 1*s* electron spectrum is shown in Fig. 1(d).

The values of the oxidized sodium core-electron binding energies are given in the second column of Table I. As mentioned for the case of the sodium metal, these values are not absolute. However, unlike sodium, whose zero energy reference level is the Fermi edge, the Fermi level in oxidized sodium is not a meaningful reference. The reason for this is that the position of the Fermi level in an insulator under x radiation, i. e., in a nonequilibrium state, is not well defined. Following a somewhat more detailed discussion,³⁰ the best that can be said about such a system is that a steady state is eventually reached whereby radiation-produced holes are filled at a rate equal to their production. This results in the stabilization of the Fermi level (or quasi-Fermi-level) in the insulator but does not necessarily imply that the sample is uncharged. In the limit of no sample charging, the number of excess holes in the system is essentially zero, resulting in alignment of Fermi levels between insulator and spectrometer. Returning to this particular system, while we cannot entirely rule out the possibility of a finite steady-state sample charge, the magnitude of such a charge may be assumed to be very small for three reasons.

First, flooding the x-radiated thin oxidized film with low-energy electrons produced no observable effect on either the width, position, or shape of any photoemission lines. Second, the core lines in the oxidized sodium are chemically shifted from those of Na by less than 1 eV, consistent with no appreciable charge accumulation. The final reason for assuming negligible sample charging is

found through comparison of the relative linewidths of the core levels in Na metal with those of the exposed film. The core-level linewidths for both systems as determined from the least-squares analysis after appropriate background subtraction and including the instrumental resolution are given in Table II. The most obvious feature in this table is that the linewidths in the oxidized sodium are considerably broader than those in the metal. The explanation of this result and its consequent implications are beyond the scope of the present study and is discussed in a separate work.³⁵ We simply mention here that the observed broadening is a lifetime effect rather than one due to some other spurious source, such as inhomogeneous sample charging. This source of broadening can be effectively ruled out since the Na 2*s* widths in the oxidized sodium are proportionately less broadened than for Na 2*p*; if charging were important, all lines would be broadened by a constant amount.

It is now appropriate to turn our attention to the valence region of the oxidized sodium film, shown in the lower portion of Fig. 8, and to discuss its identification as NaOH rather than Na₂O. The oxygen 2*s*-2*p* splitting in the free O²⁻ ion is 14.93 \pm 0.04 eV determined from a linear extrapolation of isoelectronic free-ion data.¹⁶ The value of the splitting which is closest, but certainly not equal, to this in the valence spectrum is 13.8 eV between the peak at 11.0 eV and the rather broad one at 24.8 eV. We now compare this splitting with that for water vapor, taken from Siegbahn and co-workers³⁶ and displayed in the middle third of Fig. 8. As shown, the water-vapor spectrum has been shifted to lower absolute binding energies by 7.4 eV in order to bring the peaks in coincidence. The 1*a*₁ molecular orbital (MO) in the water-vapor spectrum, composed of about 75% O 2*s* and 25%

TABLE II. Na and NaOH core-electron linewidths at FWHM (in eV).^{a,b}

	2 <i>p</i> ^c	2 <i>s</i>	1 <i>s</i> ^d
Na	0.65(3)	0.91(2)	1.47(15)
NaOH	1.49(2)	1.59(1)	1.73(10)

^aThese widths include the constant instrumental resolution of \sim 0.6 eV.

^bNumbers in parentheses correspond to uncertainties in the last digit and are the standard deviation obtained from the least-squares fit.

^cBecause Coster-Kronig filling from the 2*p*_{3/2} to 2*p*_{1/2} orbitals is either energetically forbidden or very improbable, both components have the same width.

^dThese values are somewhat unreliable because the performance of the dispersion compensation technique used in this instrument is not well characterized for binding energies above 1 keV.

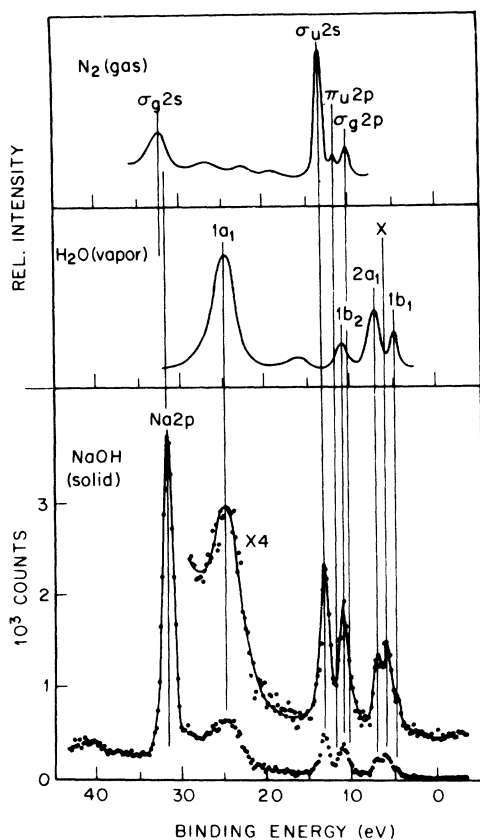


FIG. 8. (Lower) Valence band spectrum of sodium hydroxide. Molecular orbitals of spectrum are shown to be composed of those comprising water vapor (middle) and gaseous (physisorbed) nitrogen (upper). See text for details.

H 1s atomic orbital (AO) character as determined from CNDO calculations,³⁶ and the $1b_2$ MO, composed of about 60% O 2p and 40% H 1s AO character, are also split by 13.8 eV. There also appears to be good agreement in relative orbital positions between the $2a_1$ (72% O 2p, 10% O 2s, 17% H 1s) and $1b_1$ (100% O 2p) MO's and the peak observed in the oxidized sodium valence region.³⁷ The strong resemblance between these two spectra clearly suggests that the sodium metal has been oxidized to sodium hydroxide.

That the spectra are so strikingly similar is at first surprising, for we are comparing not only different species, but ones that are in different phases as well. However, based on crystal-structure data,³⁸ it is established that the strong hydrogen bonding present in NaOH renders the tetrahedral charge configuration of the hydroxyl ion virtually identical to that of the water molecule. It is also interesting to note that this result was suggested by Bernal and Megaw³⁹ more than a decade before such crystal studies were performed. The conclusion that the oxidized sodium film is

indeed NaOH is in agreement with the conditions under which it was prepared, for it is expected that the atmosphere in the plastic glove bag, although purged with dry nitrogen, contains water vapor from the adsorbed moisture on the inside plastic walls of the glove bag and diffused moisture from the outside atmosphere.

The presence of the nitrogen gas in the bag and the observance of a N 1s signal allows the assignment of molecular nitrogen gas on the exposed sodium film. This is shown in the upper third of Fig. 8. Here, we have shifted the peak positions of the MO's in the gaseous nitrogen spectrum, again taken from Siegbahn *et al.*,³⁶ by 5.5 eV. That the magnitude of this shift for nitrogen is lower than that necessary for alignment of the MO's in water vapor is interpreted as being primarily due to the smaller crystal polarization energy experienced by nitrogen. This follows if we assume that the molecular nitrogen is very weakly chemisorbed to the sodium hydroxide surface, not an unreasonable assumption based upon its relative inertness and the close resemblance of its photoemission spectrum to that of the free molecular species. It should be mentioned that the absolute magnitudes of the shifts for both N_2 and H_2O include not only the NaOH crystal polarization energy³⁰ and the difference in initial-state potentials for the free and solid-state systems,²³ but that these shifts also include the appreciably sized difference in reference levels (vacuum vs Fermi). For the NaOH system we estimate the crystal polarization for H_2O ($\sim OH^-$) to be about 2 eV, in accord with calculated values for other ions in similar crystals,³⁰ while the smaller polarization energy for N_2 is expected from the very weak interactions between a photoionized hole in it and the electrons in NaOH.

Looking at the NaOH valence band MO's somewhat more carefully, we note that while their relative positions are in good agreement with the assignments given above, their relative intensities seem to be in poorer agreement. If the intensities of the MO's are normalized to that of the $1b_1$ MO (100% O 2p), the approximate relative intensities obtained for the $2a_1$, $1b_2$, and $1a_1$ MO's are, respectively, 1.7, 0.8, and 3.2 for H_2O , and 1.8, 3.1, and 5.2 for NaOH. The greater relative intensities of the $1b_2$ and $1a_1$ MO's in NaOH can be partly explained by the expectedly less H 1s contribution in NaOH. However, we believe this effect to be only contributory, and that the major effect lies in the detailed analysis of the photoelectric cross sections of the constituent atomic orbitals in each MO.⁴⁰

In concluding discussion of the NaOH valence band spectrum, we focus attention on the unassigned peak, labeled X, located between the $2a_1$ and $1b_1$ MO's at 6.0 eV. Its origin may be thought

to arise from several sources. One source is from possibly existing oxygen-containing carbon impurities, e.g., CO or CO₂. We have looked at the C 1s signal during the course of the experiments on the sodium metal and have found weak signals (C-1s-Na-1s intensity ratio, after the Z^4 correction, was 0.011), but unfortunately do not have similar C 1s data for the exposed sodium film. It may be argued, however, that if this were the source, the NaOH valence band would certainly contain additional structure from the other carbon-oxygen MO's. Another possible and somewhat intriguing explanation for this extra peak may be seen by inspection of the NaOH crystal structure with the positions of the H atoms assigned by Busing.⁴¹ From this it is revealed that the H atoms on the *c*-axis OH⁻ ions that are on the surface are directed away from the bulk NaOH in such a way that hydrogen bonding is no longer possible. We therefore tentatively attribute the source of this extra peak as arising from the nonbonding O 2*p* atomic orbitals on those hydroxyl ions which are directly on the surface. Assuming this were

the case, the formerly nondegenerate 2*a*₁ and 1*b*₁ orbitals would be degenerate, and the resulting orbital would have an energy intermediate between those of its formerly nondegenerate constituents with an intensity approximately equal to their sum. This is, in fact, what is observed. Before any firm conclusions may be drawn, however, a careful surface investigation of this system under more controlled contamination conditions is clearly required.

ACKNOWLEDGMENTS

I am pleased to acknowledge H. E. Weaver and L. H. Scharpen of the Hewlett-Packard Scientific Instrument Division for their help in obtaining the data, and to Hewlett-Packard for allowing the opportunity to use their spectrometer. Helpful comments and suggestions from M. B. Robin, J. E. Rowe, N. V. Smith, and G. K. Wertheim are also gratefully acknowledged. I am indebted to D. R. Hamann for numerous stimulating discussions and for his critical review of the manuscript.

¹E. Wigner and F. Seitz, *Phys. Rev.* **43**, 804 (1933).

²K. Siegbahn, C. Nordling, A. Fahlman, R. Nordberg, K. Hamrin, J. Hedman, G. Johansson, T. Bergmark, S. E. Karlsson, I. Lindgren, and B. Lindberg, *ESCA-Atomic, Molecular, and Solid State Structure by Means of Electrons Spectroscopy* (Almqvist and Wiksells, Uppsala, Sweden, 1967).

³*Electron Spectroscopy*, edited by D. A. Shirley (North-Holland, Amsterdam, 1972).

⁴For further description, see K. Siegbahn, D. Hammond, H. F. Feldegg, and E. F. Barnett, *Science* **176**, 245 (1972).

⁵R. A. Pollak, Lawrence Radiation Laboratory Report No. LBL-1299, 1972 (unpublished).

⁶M. S. A. Research Corp., Division of Mine, Safety, Appliance Corp., Evans City, Pa.

⁷For example, see R. G. Steinhardt, J. Hudis, and M. L. Perlman, *Ref. 3*, p. 557.

⁸P. H. Citrin and D. R. Hamann (unpublished).

⁹Y. Baer and G. Busch, *Phys. Rev. Lett.* **30**, 280 (1973).

¹⁰A. Barrie, *Chem. Phys. Lett.* **19**, 109 (1973).

¹¹A. H. Compton and S. K. Allison, *X-Rays in Theory and Experiment*, 2nd ed. (MacMillan, London, 1935), p. 533.

¹²J. C. Tracy, in *Proceedings of NATO Conference on Electron Emission Spectroscopy*, Ghent, Belgium, 1972 (unpublished).

¹³The difference in thickness between a sodium metal and a sodium hydroxide monolayer is negligibly small.

¹⁴M. J. G. Lee, *Crit. Rev. Solid State Sci.* **85** (1971).

¹⁵The relative merits of these techniques are discussed more thoroughly by S. Hüfner, G. K. Wertheim, and J. H. Wernick, *Phys. Rev. B* (to be published).

¹⁶C. E. Moore, *Atomic Energy Levels*, Natl. Bur. Std. Circ. No. 467 (U. S. GPO, Washington, D. C., 1949).

¹⁷J. B. Swan, *Phys. Rev.* **135**, A1467 (1964).

¹⁸C. Kunz, *Phys. Lett.* **15**, 312 (1965).

¹⁹R. H. Ritchie, *Phys. Rev.* **106**, 874 (1957).

²⁰E. A. Stern and R. A. Ferrel, *Phys. Rev.* **120**, 130 (1960).

²¹G. J. Van Oirschot, M. van den Brink, and W. M. H. Sachtler, *Surf. Sci.* **29**, 189 (1972), and references cited therein.

²²Yu. I. Malov, V. B. Lazarev, and A. V. Salov, *Izv. Akad. Nauk SSSR Ser. Khim.* 2121 (1970).

²³P. H. Citrin and D. R. Hamann, *Chem. Phys. Lett.* **22**, 301 (1973).

²⁴G. D. Mahan, *Phys. Rev.* **163**, 612 (1967).

²⁵P. Nozières and C. T. de Dominicis, *Phys. Rev.* **178**, 1097 (1969).

²⁶S. Doniach and M. Šunjić, *J. Phys. C* **3**, 285 (1970).

²⁷S. Doniach, *Phys. Rev. B* (to be published) and references cited therein.

²⁸L. Hedin, *Ark. Fys.* **30**, 231 (1965).

²⁹The difference between (2*p*, 3*s*) electron correlation energies in these two systems is negligibly small.

³⁰P. H. Citrin and T. D. Thomas, *J. Chem. Phys.* **57**, 4446 (1972).

³¹C. S. Fadley, S. B. M. Hagström, M. P. Klein, and D. A. Shirley, *J. Chem. Phys.* **48**, 3779 (1968).

³²H. W. Wolff, K. Radler, B. Sonntag, and R. Haensel, *Z. Phys.* **257**, 353 (1972).

³³C. Zener, *Phys. Rev.* **36**, 51 (1930).

³⁴J. C. Slater, *Phys. Rev.* **36**, 57 (1930).

³⁵P. H. Citrin, *Phys. Rev. Lett.* **31**, 1164 (1973).

³⁶K. Siegbahn, C. Nordling, G. Johansson, J. Hedman, P. F. Hedén, K. Hamrin, U. Gelius, T. Bergmark, L. O. Werme, R. Manne, and Y. Baer, *ESCA Applied to Free Molecules* (North-Holland, Amsterdam, 1969).

³⁷These orbital assignments were based on data taken over a narrower energy range (0–10 eV) with sufficient statistics to permit such assignments.

³⁸T. Ernst, *Nachr. Ges. Wiss. Goett. Math.-Phys. Kl.* **76** (1946); T. Ernst and R. Schober, *Nachr. Ges. Wiss. Goett. Math.-Phys. Kl.* **49** (1947); T. Ernst, *Angew. Chem. (Int. Ed. Engl.)* **60A**, 77 (1948).

³⁹J. D. Bernal and H. D. Megaw, *Proc. R. Soc. A* **151**, 384 (1935).

⁴⁰For a good discussion of these procedures, see U. Gelius, in *Ref. 3*, p. 311; U. Gelius, C. J. Allen, G. Johansson, H. Siegbahn, D. A. Allison, and K. Siegbahn, *Phys. Scr.* **3**, 237 (1971); U. Gelius, C. J. Allen, D. A. Allison, H. Siegbahn, and K. Siegbahn, *Chem. Phys. Lett.* **11**, 224 (1971). Also, see L. L. Lohr and M. B. Robin, *J. Am. Chem. Soc.* **92**, 7241 (1970).

⁴¹W. R. Busing, *J. Chem. Phys.* **23**, 933 (1955).

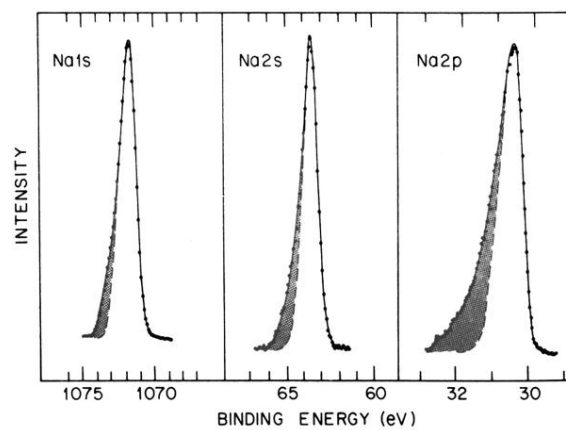


FIG. 6. Evidence for conduction-electron excitations from core holes. The effect, shown as shaded asymmetric broadening, is more obvious for the narrower peaks of the long-lived core electrons. Note the different energy scales for each core electron.